

1 The origin and maintenance of metabolic allometry in animals

2

3 Craig R. White^{1,2,*}, Dustin J. Marshall², Lesley A. Alton^{1,2}, Pieter A. Arnold^{1,3}, Julian E. Beaman¹,
4 Candice L. Bywater^{2,4}, Catriona Condon⁵, Taryn S. Crispin¹, Aidan Janetzki¹, Elia Pirtle⁴,
5 Hugh S. Winwood-Smith¹, Michael J. Angilletta Jr.⁵, Stephen F. Chenoweth¹, Craig E.
6 Franklin¹, Lewis G. Halsey⁶, Michael R. Kearney⁴, Steven J. Portugal⁷, Daniel Ortiz-Barrientos¹

7

8 ¹School of Biological Sciences, The University of Queensland, Queensland, Australia 4072

9 ²Centre for Geometric Biology, School of Biological Sciences, Monash University, Victoria,
10 Australia, 3800.

11 ³Research School of Biology, The Australian National University, Acton, Australian Capital
12 Territory, Australia 2601

13 ⁴School of Biosciences, The University of Melbourne, Parkville Campus, Victoria, Australia,
14 3010

15 ⁵School of Life Sciences, Arizona State University, Tempe, Arizona 85287, USA

16 ⁶Department of Life Sciences, University of Roehampton, Holybourne Avenue, London
17 SW15 4JD, UK

18 ⁷School of Biological Sciences, Royal Holloway, University of London, Egham, Surrey,
19 TW20 0EX, UK

20

21 *e-mail: craig.white@monash.edu

22

23 **Organisms vary widely in size from microbes weighing 0.1 picograms to trees weighing**
24 **thousands of megagrams, a 10²¹-fold range similar to the difference in mass between**
25 **an elephant and the Earth. Mass has a pervasive influence on biological processes but**
26 **the effect is usually non-proportional; for example, a 10-fold increase in mass is**
27 **typically accompanied by just a 4-to-7-fold increase in metabolic rate. Understanding**
28 **the cause of allometric scaling has been a long-standing problem in biology. Here, we**
29 **examine the evolution of metabolic allometry in animals by linking microevolutionary**
30 **processes to macroevolutionary patterns. We show that the genetic correlation**
31 **between mass and metabolic rate is strong and positive in insects, birds, and mammals.**
32 **We then use these data to simulate the macroevolution of mass and metabolic rate, and**
33 **show that the interspecific relationship between these traits in animals is consistent**
34 **with evolution under persistent multivariate selection on mass and metabolic rate over**
35 **long periods of time.**

36 Animals expend energy to survive, forage, grow, and reproduce, and the processes that
37 cause variation in metabolic rate have fascinated biologists for over a century¹⁻¹¹. Metabolic
38 rates integrate many organismal functions¹², and relate to several traits that enhance fitness
39 (e.g., social dominance, offspring growth, and lifetime reproductive success^{8,13-15}). Because
40 energy turnover varies according to size, measurements of metabolic rate (MR) and body
41 mass (M) are usually strongly correlated. Among species of birds and mammals, for example,
42 more than 94% of the variance in MR can be explained by M alone¹⁶⁻¹⁸. Surprisingly, however,
43 MR is not linearly proportional to M ; instead, MR is proportional to M^b , where b is typically
44 less than one^{6,9}, especially for resting MR and daily mean MR of free-living animals¹⁹; b is
45 often higher and can approach isometry ($b=1$) for maximally-active animals⁷. Mechanistic
46 hypotheses proposed to explain the observed relationships between MR and M have invoked
47 variation in a range of physical constraints such as the geometry of circulatory networks^{4,5},
48 the need to dissipate heat^{7,20}, or surface area-volume ratios that influence the flux of nutrients
49 or wastes²¹⁻²³. Other approaches that explain variation in metabolic scaling have invoked
50 biotic and abiotic drivers such as lifestyle and temperature²⁴, foraging²⁵, predation²⁶, and a
51 range of others^{7-9,27,28}, or differences in body size optimization and the distributions of
52 intraspecific production and mortality parameters across species²⁹. Here we complement
53 these studies by investigating microevolutionary and macroevolutionary processes
54 responsible for variation in scaling of metabolic rate in animals.

55 Theory predicts that microevolutionary processes can lead to macroevolutionary
56 associations between MR and M in at least two ways:

57 1. Metabolic allometry could arise due to constraints in the genetic architecture of
58 traits, with little to no role for selection coupled with random evolution³⁰. When two traits
59 share genetic variance, through pleiotropy, they do not evolve independently³¹ thus the
60 evolution of MR and M could be constrained if the two traits are genetically correlated. Under
61 this scenario, a macroevolutionary relationship between MR and M is expected to arise and
62 persist even in the absence of selection.

63 2. Metabolic allometry could also arise through correlational selection increasing the
64 covariance between MR and M ^{30,32}. Under this model, natural selection favours particular
65 combinations of MR and M over others, and it is the pattern of multivariate selection that
66 gives rise to the sub-linear scaling of MR with M . This model implies that fitness would differ
67 between individuals with the same mass-specific MR ($= MR/M$) and different M ; fitness would
68 be highest for small individuals with high mass-specific MR and for large individuals with low
69 mass-specific MR .

70 To distinguish between these two explanations (hereafter random evolution, and
71 correlational selection), we took a three-pronged approach: first, we estimated the
72 distribution and strength of the genetic correlation between MR and M for a suite of species
73 across 800 million years of animal evolution. Using the distribution of genetic correlations
74 between MR and M and the distributions of the genetic variances of these traits, we next
75 simulated repeatedly the evolution of MR and M along a phylogeny. This process generated a
76 distribution of values for each of these traits, from which we could calculate the variation in
77 both the scaling exponent of MR and the magnitude of residual variation in MR (the variation
78 in MR that is not explained by variation in M). We then compared the distributions of the
79 simulated data with empirical data. If the distribution of simulated values of the scaling
80 exponent b and the distribution of simulated residual (mass-independent) variation in MR
81 both match their empirical distributions, the allometric scaling of MR with M could have
82 resulted from random evolution. If, on the other hand, the distribution of simulated values of
83 b does not match the empirical distribution, or if the simulated residual variation of MR is
84 greater than that of the empirical data, this would demonstrate that the allometric scaling of
85 MR with M is instead consistent with evolution under correlational selection.

86 Results

87 As was the case in previous studies of birds³³⁻³⁵ and mammals³⁶, our own empirical
88 estimates for three species of insects revealed that the genetic correlation (r_G) between M and
89 resting MR is positive and strong (Fig. 1). In a previous study of speckled cockroaches
90 *Nauphoeta cinerea*³⁷, we determined the additive genetic correlation using a paternal half
91 sibling-full sibling breeding design ($n = 637$ individuals; 48 half-sibling families, 126 full-
92 sibling families). In a previous study of fruit flies *Drosophila melanogaster* ($n = 247$
93 individuals), we measured the metabolic rates and dry body masses of 85 isofemale lines³⁸. In
94 the present study, we measured metabolic rates and body masses of 438 individual
95 *Drosophila serrata* from 45 isofemale lines created from natural populations. For both species
96 of *Drosophila*, we determined genetic correlations among isofemale lines (see Supplementary
97 Information for details). For all three species of insect, a strong positive genetic correlation
98 was observed (*Nauphoeta cinerea* males: 0.98 ± 0.18 [SE], females: 0.50 ± 0.37 ; *Drosophila*
99 *melanogaster*: 0.48 ± 0.17 ; *Drosophila serrata*: 0.99 ± 0.17). For the full data set including
100 birds and mammals, r_G values range from 0.40 ± 0.35 to 1.18 ± 0.46 (Fig. 1).

101 To evaluate theoretical predictions, we first explored whether random evolution could
102 have produced the observed distribution of interspecific scaling exponents (b). We simulated

103 the evolution of MR and M along phylogenies (e.g. Fig. 2), and compared our simulated data
104 with an empirical distribution of b estimated from 4,794 means of MR and M for 2,168 species.
105 These data include 3,799 of our own measurements of MR for 2,936 individuals of 32 species
106 in addition to those compiled from the literature (all data are provided in the Supplementary
107 Material).

108 The empirical estimates of b for resting, free-living, and active animals (Supplementary
109 Figure 1) fall within the simulated distribution based on the genetic correlation between MR
110 and M and their genetic variances (Figs 3a,b). The empirical values for the residual variances
111 also fall within the simulated distribution (Fig. 3c,d). The tails of the simulated distributions
112 are long (Fig. 3), however, and the 95% density contour of the simulated data includes regions
113 of parameter space far outside of the narrow region occupied by the empirical data (Fig. 4).
114 The relationship between MR and M is therefore far more constrained than expected by
115 chance, and we conclude that the macroevolutionary relationship between MR and M arises as
116 a consequence of correlational selection on these traits. This conclusion is robust to the
117 underlying distribution of the ratio of σ_{MR}^2 to σ_M^2 used in the simulations (Supplementary
118 Figures 2-4)

119 Discussion

120 Theory predicts that responses to selection on a trait initially depend on the genetic
121 correlations between traits, but they are determined by a balance between the intensities of
122 stabilizing and directional selection over longer time scales³². Genetic correlations can arise
123 by chance³⁹ and as a consequence of multivariate selection⁴⁰⁻⁴². We hypothesise that the
124 apparent persistence of the genetic correlation between MR and M over at least some narrow
125 regions of the tree of life suggests that multivariate selection is likely responsible for the
126 distribution of genetic correlations observed in extant species (Fig. 1). Such multivariate
127 selection acting on MR and M could also act to constrain the observed distributions of these
128 traits, restricting the empirical distributions of b and residual variances to the narrow range
129 observed relative to simulations (Fig. 4). Genetic correlations can vary among
130 environments⁴³, as can intraspecific metabolic scaling relationships^{24,26,27,44}, and so
131 comparisons of the genetic (co)variances of MR and M for animals reared or evolved in
132 multiple environments would also be valuable and might provide insight into how the
133 strength and direction of multivariate selection varies among environments. Such data may be
134 particularly useful in explaining the shifts in metabolic scaling that are observed across the
135 tree of life¹¹.

136 Multivariate selection on *MR* and *M* could result from physical constraints associated
137 with nutrient mobilisation^{23,45,46}, nutrient transport^{4,5}, heat dissipation^{7,20}, the exchange of
138 nutrients or wastes across surfaces^{21,22}, or combinations of these acting on different
139 combinations of *MR* and *M*. Variation in the relative contribution of these physical constraints,
140 or their mediation by environmental context, might also contribute to variation in the scaling
141 exponent of metabolic rate^{8,23,45,46}. Yet despite the considerable interest in these mechanistic
142 hypotheses, variation in these functional characteristics of organisms have not been
143 empirically linked to measurements of fitness, either directly or indirectly via variation in *MR*;
144 indeed, measurements of the link between lifetime reproductive success and *MR* are
145 exceedingly rare¹⁰. Future work could fill this knowledge gap by examining how the putative
146 mechanistic drivers of metabolic scaling determine the functional basis of variation in fitness.

147 Our results show that interspecific relationship between metabolic rate and body mass
148 in animals is consistent with evolution under persistent multivariate selection. The strong
149 positive genetic correlation between *MR* and *M* is present in species of insect, bird, and
150 mammal spanning around 800 million years of evolution (Fig. 1) and might have arisen as a
151 consequence of persistent multivariate selection. These factors – random evolution,
152 multivariate selection, and a persistent genetic correlation – link the micro- and macro-
153 evolution of *MR* and *M* thereby explaining the multivariate distributions of these fundamental
154 traits across the animal tree of life (Fig. 5): microevolutionary processes dictate the trait space
155 available to organisms, and macroevolutionary patterns describe the regions of trait space
156 that are selected over long periods of time.

157 **Methods**

158 *Measurements of metabolic rates*

159 Metabolic rates were measured using standard positive pressure flow-through
160 respirometry⁴⁷, using techniques that are described in detail elsewhere (e.g. ^{37,38}) and in the
161 supplementary material. Briefly, air was scrubbed of CO₂ and water vapour before being
162 passed at a known flow rate through a chamber containing an animal, and the concentration
163 of CO₂, or the concentrations of O₂ and CO₂, were measured in the excurrent air. Rates of CO₂
164 production and O₂ consumption were then calculated using standard equations⁴⁷. For systems
165 in which only CO₂ was measured, rates of CO₂ production were converted to rates of O₂
166 consumption assuming a respiratory exchange ratio (RER) of 0.8 (RER = rate of CO₂
167 production divided by rate of O₂ production).

168 *Determination of genetic correlations*

169 For *Drosophila serrata*, genetic (among-line) correlations between body mass and
170 metabolic rate, conditioned on activity and age (ref⁴⁸), were calculated using ASReml-R v3.0
171 (ref⁴⁹) in R v2.0.2. Approximate standard errors for the estimate of the genetic correlation
172 were calculated using the R ‘pin’ function⁵⁰. For *Drosophila melanogaster*, genetic (among-
173 line) correlations between dry body mass and metabolic rate, conditioned on temporal block,
174 population, and measurement temperature (ref⁴⁸), were calculated.

175 *Simulations of trait evolution*

176 We simulated the evolution of $\log_{10}M$ and $\log_{10}MR$ over randomly generated
177 phylogenies with 4,000 tips using the ‘pbtrees’ function of the phytools⁵¹ package in R⁵².
178 Preliminary analyses showed that the results were qualitatively similar when larger trees
179 were used, but processing time was considerably increased; we therefore selected a value of
180 4,000 tips because it is similar to the number of extant species of mammal. Results were also
181 similar if a real tree with branch lengths in units of time was used⁵³. We simulated trait values
182 using the ‘sim.corr’ function of phytools to conduct Brownian motion simulation on a tree
183 with evolutionary correlations between characters⁵¹. We set the starting values for the
184 simulation as the medians of \log_{10} -transformed M and basal MR for mammals⁵⁴; the simulated
185 distributions of b and mass-independent MR are unaffected by these starting values, which
186 influence only the means of $\log_{10}M$ and $\log_{10}MR$ for the simulated data, not their
187 (co)variances. We set the variance for $\log_{10}M$ (σ_M^2) at 0.025 to yield simulated body masses for
188 extant taxa at the tip of the tree that span a biologically realistic range. We calculated the
189 variance for $\log_{10}MR$ (σ_{MR}^2) based on a distribution of 100,000 values generated using a
190 Weibull distribution (shape = 3.23, scale = 0.818) fitted to the empirical distribution of four
191 values of the ratio of σ_{MR}^2 to σ_M^2 calculated using log-log transformed data for *Drosophila*
192 *serrata* (0.81), *Drosophila melanogaster* (0.55), and male and female *Nauphoeta cinerea* (1.1
193 and 0.47, respectively). We set covariances at $r_G\sqrt{\sigma_{MR}^2}\sqrt{\sigma_M^2}$, where we generated a distribution
194 of 100,000 values of r_G based on the distribution of Fisher’s Z-transformed values of r_G for
195 extant species (mean $Z = 1.55$, s.d. = 1.18, $n = 9$; for Z-transformation, estimates of $r_G \geq 1$ were
196 substituted with values of 0.999; there was no systematic difference between estimates of Z
197 calculated using log-transformed or untransformed data [$t_7 = 0.156$, $p = 0.86$], and so all data
198 were pooled). In each simulation, traits evolved randomly by Brownian motion along the tree
199 (e.g., Fig. 2), and we replicated the simulation 100,000 times.

200 *Compilation of comparative data for body mass and metabolic rate*

201 To test the predictions of our simulations, we assembled a database of body mass and
202 metabolic rate data, which includes measurements of resting animals (basal metabolic rate⁵⁵
203 for birds and mammals, standard metabolic rate⁵⁵ for insects, fish, amphibians, and reptiles),
204 free-living animals (daily energy expenditure⁵⁶ for reptiles, birds, and mammals) and animals
205 exercising at or near their aerobic limits in a laboratory setting (maximum aerobic metabolic
206 rate⁵⁷ for terrestrial mammals and cursorial birds, maximum rate of oxygen uptake for fish⁵⁸,
207 and *MR* during flight for insects, bats, and birds). In addition to our measurements of
208 metabolic rate (Supplementary Table 1), we assembled published databases and generated
209 new compilations where published databases were not available (Supplementary Table 2).

210 For our new compilations of insect standard metabolic rate (Supplementary Table 3)
211 and flight metabolic rate (Supplementary Table 4), reptile field metabolic rate
212 (Supplementary Table 5), and bird field metabolic rate (Supplementary Table 6) and
213 maximum metabolic rate (Supplementary Table 7), we searched online databases (Google
214 Scholar and Web of Science) using key words that identified the measurements of interest
215 (“metabolic rate” or “rate of oxygen consumption” or “rate of carbon dioxide production” or
216 respirometry or calorimetry or “doubly labelled water” or “daily energy expenditure” or
217 “aerobic capacity”). For each of the records identified by this search, we first scanned the title
218 to determine if a record was likely to contain data or citations to data. If the title was
219 promising, we reviewed the abstract, and if that was promising we reviewed the full text. For
220 each record that was reviewed at the full text level, we also searched for cited papers that
221 might contain data. We did not, unfortunately, maintain a tally of how many records were
222 retrieved or how many papers were reviewed at each level. The full database of metabolic
223 rates includes species that vary in size from ants to elephants (0.1 milligrams - 2.6
224 megagrams). Metabolic rates ranged from 35 picolitres of O₂ per minute for resting weevils
225 (0.5 mg) to 3.6 litres of O₂ per minute for exercising horses (450 kg).

226 *Determination of empirical scaling exponents*

227 We calculated the scaling exponent of metabolic rate, *b*, for each taxonomic group
228 (insects, fish, amphibians, reptiles, birds, and mammals) and each metabolic state (resting,
229 free-living, and exercising) using phylogenetic mixed models⁵⁹⁻⁶¹ with phylogenetic
230 relationships from v3 of the open tree of life⁶². We implemented phylogenetic mixed models
231 using ASReml-R v3.0 (ref ⁴⁹) and R v3.0.2, with inverse relatedness matrices calculated from
232 phylogenetic covariance matrices using the MCMCglmm package v2.21 ⁶³. Models for
233 endotherms and free-living reptiles included $\log_{10}MR$ as a response and $\log_{10}M$ as a predictor,

234 and all other models for ectotherms included $\log_{10}MR$ as a response and both $\log_{10}M$ and
235 measurement temperature as predictors. The parameter estimate for $\log_{10}M$ in each of these
236 models represents the scaling exponent of MR (see ref ⁹).

237 **Data Availability Statement**

238 All data generated or analysed during this study are included in this published article
239 (and its supplementary information files).

240 **Acknowledgements**

241 This research was supported by the Australian Research Council (projects
242 DP110101776, FT130101493, DP170101114, DP180103925).

243 **Author Contributions**

244 C.R.W., D.O.-B., and D.J.M. designed the study. C.R.W., L.A.A., P.A.A., J.E.B., C.L.B., C.C.,
245 T.S.C., A.J., E.P., H.S.W.-S., M.J.A., S.F.C., C.E.F., L.G.H., M.R.K., and S.J.P. collected data. C.R.W.
246 analysed data. C.R.W. and D.O.B. wrote the first version of the manuscript, and all authors
247 contributed to and approved the final version.

248 **Declaration of Competing Interests**

249 The authors declare no competing interests.

250 **References**

- 251 1 Vernon, H. M. The physiological evolution of the warm-blooded animal. *Sci. Prog.* **7**, 378
252 (1898).
- 253 2 Krogh, A. *Respiratory exchange of animals and man*. (Longmans, Green and Co., 1916).
- 254 3 Schmidt-Nielsen, K. *Scaling: Why is animal size so important?*, (Cambridge University
255 Press, 1984).
- 256 4 West, G. B., Brown, J. H. & Enquist, B. J. A general model for the origin of allometric
257 scaling laws in biology. *Science* **276**, 122-126 (1997).
- 258 5 West, G. B., Brown, J. H. & Enquist, B. J. The fourth dimension of life: Fractal geometry
259 and allometric scaling of organisms. *Science* **284**, 1677-1679 (1999).
- 260 6 Glazier, D. S. Beyond the '3/4-power law': variation in the intra- and interspecific
261 scaling of metabolic rate in animals. *Biological Reviews* **80**, 1-52 (2005).
- 262 7 Glazier, D. S. A unifying explanation for diverse metabolic scaling in animals and plants.
263 *Biological Reviews* **85**, 111-138 (2010).
- 264 8 White, C. R. & Kearney, M. R. Determinants of inter-specific variation in basal metabolic
265 rate. *J. Comp. Physiol. B* **183**, 1-26 (2013).
- 266 9 White, C. R. & Kearney, M. R. Metabolic scaling in animals: methods, empirical results,
267 and theoretical explanations. *Comprehensive Physiology* **4**, 231-256 (2014).
- 268 10 Pettersen, A. K., Marshall, D. J. & White, C. R. Understanding variation in metabolic rate.
269 *J. Exp. Biol.* **221**, jeb166876 (2018).

- 270 11 Uyeda, J. C., Pennell, M. W., Miller, E. T., Maia, R. & McClain, C. R. The evolution of
271 energetic scaling across the vertebrate tree of life. *Am. Nat.* **190**, 185-199,
272 doi:10.1086/692326 (2017).
- 273 12 Brown, J. H., Gillooly, J. F., Allen, A. P., Savage, V. M. & West, G. B. Toward a metabolic
274 theory of ecology. *Ecology* **85**, 1771-1789 (2004).
- 275 13 Burton, T., Killen, S. S., Armstrong, J. D. & Metcalfe, N. B. What causes intraspecific
276 variation in resting metabolic rate and what are its ecological consequences? *Proc. R.*
277 *Soc. Lond. B Biol. Sci.* **278**, 3465-3473, doi:10.1098/rspb.2011.1778 (2011).
- 278 14 Biro, P. A. & Stamps, J. A. Do consistent individual differences in metabolic rate
279 promote consistent individual differences in behavior? *Trends Ecol. Evol.* **25**, 653-659,
280 doi:DOI: 10.1016/j.tree.2010.08.003 (2010).
- 281 15 Pettersen, A. K., White, C. R. & Marshall, D. J. Metabolic rate covaries with fitness and
282 the pace of the life history in the field. *Proc. R. Soc. Lond. B Biol. Sci.* **283**, 20160323
283 (2016).
- 284 16 McNab, B. K. Ecological factors affect the level and scaling of avian BMR. *Comp.*
285 *Biochem. Physiol. A* **152**, 22-45 (2009).
- 286 17 McNab, B. K. An analysis of the factors that influence the level and scaling of
287 mammalian BMR. *Comp. Biochem. Physiol. A* **151**, 5-28 (2008).
- 288 18 Kolokotronis, T., Savage, V. M., Deeds, E. J. & Fontana, W. Curvature in metabolic
289 scaling. *Nature* **464**, 753-756 (2010).
- 290 19 White, C. R., Phillips, N. F. & Seymour, R. S. The scaling and temperature dependence of
291 vertebrate metabolism. *Biology Letters* **2**, 125-127 (2006).
- 292 20 Speakman, J. R. & Król, E. Maximal heat dissipation capacity and hyperthermia risk:
293 neglected key factors in the ecology of endotherms. *J. Anim. Ecol.* **79**, 726-746 (2010).
- 294 21 Speakman, J. R., McDevitt, R. M. & Cole, K. R. Measurement of basal metabolic rates:
295 Don't lose sight of reality in the quest for comparability. *Physiol. Zool.* **66**, 1045-1049
296 (1993).
- 297 22 Hirst, A. G., Glazier, D. S. & Atkinson, D. Body shape shifting during growth permits
298 tests that distinguish between competing geometric theories of metabolic scaling. *Ecol.*
299 *Lett.* **17**, 1274-1281, doi:10.1111/ele.12334 (2014).
- 300 23 Kooijman, S. A. L. M. *Dynamic Energy Budget Theory for Metabolic Organisation*. 3rd
301 edn, (Cambridge University Press, 2010).
- 302 24 Killen, S. S., Atkinson, D. & Glazier, D. S. The intraspecific scaling of metabolic rate with
303 body mass in fishes depends on lifestyle and temperature. *Ecol. Lett.* **13**, 184-193
304 (2010).
- 305 25 Witting, L. The body mass allometries as evolutionarily determined by the foraging of
306 mobile organisms. *J. Theor. Biol.* **177**, 129-137, doi:10.1006/jtbi.1995.0231 (1995).
- 307 26 Glazier, D. S. *et al.* Ecological effects on metabolic scaling: amphipod responses to fish
308 predators in freshwater springs. *Ecol. Monogr.* **81**, 599-618, doi:10.1890/11-0264.1
309 (2011).
- 310 27 Glazier, D. S. Beyond the '3/4-power law': variation in the intra- and interspecific
311 scaling of metabolic rate in animals. *Biological Reviews* **80**, 622-662 (2005).
- 312 28 Glazier, D. S. Is metabolic rate a universal 'pacemaker' for biological processes?
313 *Biological Reviews*, n/a-n/a, doi:10.1111/brv.12115 (2014).
- 314 29 Kozłowski, J. & Weiner, J. Interspecific allometries are by-products of body size
315 optimization. *Am. Nat.* **149**, 352-380 (1997).
- 316 30 Lande, R. Quantitative genetic analysis of multivariate evolution, applied to brain: body
317 size allometry. *Evolution* **33**, 402-416 (1979).
- 318 31 Walsh, B. & Blows, M. W. Abundant genetic variation + strong selection = Multivariate
319 genetic constraints: A geometric view of adaptation. *Annual Review of Ecology*,

320 *Evolution, and Systematics* **40**, 41-59, doi:10.1146/annurev.ecolsys.110308.120232
321 (2009).

322 32 Zeng, Z.-B. Long-term correlated response, interpopulation covariation, and
323 interspecific allometry. *Evolution* **42**, 363-374, doi:10.2307/2409239 (1988).

324 33 Tieleman, B. I., Versteegh, M. A., Helm, B. & Dingemanse, N. J. Quantitative genetics
325 parameters show partial independent evolutionary potential for body mass and
326 metabolism in stonechats from different populations. *Journal of Zoology* **278**, 129-136
327 (2009).

328 34 Nilsson, J.-Å., Åkesson, M. & Nilsson, J. F. Heritability of resting metabolic rate in a wild
329 population of blue tits. *J. Evol. Biol.* **22**, 1867-1874 (2009).

330 35 Ronning, B., Jensen, H., Moe, B. & Bech, C. Basal metabolic rate: heritability and genetic
331 correlations with morphological traits in the zebra finch. *J. Evol. Biol.* **20**, 1815-1822,
332 doi:10.1111/j.1420-9101.2007.01384.x (2007).

333 36 Careau, V. *et al.* Genetic correlation between resting metabolic rate and exploratory
334 behaviour in deer mice (*Peromyscus maniculatus*). *J. Evol. Biol.* **24**, 2153-2163 (2011).

335 37 Schimpf, N. G., Matthews, P. G. D. & White, C. R. Discontinuous gas exchange exhibition
336 is a heritable trait in speckled cockroaches *Nauphoeta cinerea* *J. Evol. Biol.* **26**, 1588-
337 1597 (2013).

338 38 Alton, L. A., Condon, C., White, C. R. & Angilletta, M. J., Jr. Colder environments did not
339 select for a faster metabolism during experimental evolution of *Drosophila*
340 *melanogaster*. *Evolution* **71**, 145-152, doi:10.1111/evo.13094 (2017).

341 39 Nespolo, R. F. & Roff, D. A. Testing the aerobic model for the evolution of endothermy:
342 implications of using present correlations to infer past evolution. *Am. Nat.* **183**, 74-83,
343 doi:10.1086/674093 (2014).

344 40 Delph, L. F., Steven, J. C., Anderson, I. A., Herlihy, C. R. & Brodie III, E. D. Elimination of a
345 genetic correlation between the sexes via artificial correlational selection. *Evolution*
346 **65**, 2872-2880, doi:10.1111/j.1558-5646.2011.01350.x (2011).

347 41 Roff, D. A. & Fairbairn, D. J. A test of the hypothesis that correlational selection
348 generates genetic correlations. *Evolution* **66**, 2953-2960, doi:10.1111/j.1558-
349 5646.2012.01656.x (2012).

350 42 Roff, D. A. & Fairbairn, D. J. The evolution of trade-offs under directional and
351 correlational selection. *Evolution* **66**, 2461-2474, doi:10.1111/j.1558-
352 5646.2012.01634.x (2012).

353 43 Sgrò, C. M. & Hoffmann, A. A. Genetic correlations, tradeoffs and environmental
354 variation. *Heredity* **93**, 241-248, doi:10.1038/sj.hdy.6800532 (2004).

355 44 Glazier, D. S. The 3/4-power law is not universal: evolution of isometric, ontogenetic
356 metabolic scaling in pelagic animals. *Bioscience* **56**, 325-332 (2006).

357 45 Kooijman, S. A. L. M. Energy budgets can explain body size relations. *J. Theor. Biol.* **121**,
358 269-282, doi:10.1016/s0022-5193(86)80107-2 (1986).

359 46 Maino, J. L., Kearney, M. R., Nisbet, R. M. & Kooijman, S. A. L. M. Reconciling theories for
360 metabolic scaling. *J. Anim. Ecol.*, DOI: 10.1111/1365-2656.12085, doi:10.1111/1365-
361 2656.12085 (2013).

362 47 Lighton, J. R. B. *Measuring metabolic rates: a manual for scientists*. (Oxford University
363 Press, 2008).

364 48 Wilson, A. J. Why h^2 does not always equal V_A/V_P ? *J. Evol. Biol.* **21**, 647-650 (2008).

365 49 Gilmour, A. R., Gogel, B. J., Cullis, B. R. & Thompson, R. *ASReml user guide. Release 3.0*.
366 (NSW Department of Industry and Investment, 2009).

367 50 White, I. R pin function. <http://www.homepages.ed.ac.uk/iwhite//asreml/>. (2013).

368 51 Revell, L. J. phytools: an R package for phylogenetic comparative biology (and other
369 things). *Methods in Ecology and Evolution* **3**, 217-223 (2012).

370 52 R: A Language and Environment for Statistical Computing. v. 3.2.2 (R Foundation for
371 Statistical Computing, Vienna, Austria, 2016).

372 53 Bininda-Emonds, O. R. P. *et al.* The delayed rise of present-day mammals. *Nature* **446**,
373 507-512 (2007).

374 54 Jones, K. E. *et al.* PanTHERIA: a species-level database of life history, ecology, and
375 geography of extant and recently extinct mammals. *Ecology* **90**, 2648 (2009).

376 55 Frappell, P. B. & Butler, P. J. Minimal metabolic rate, what it is, its usefulness, and its
377 relationship to the evolution of endothermy: a brief synopsis. *Physiol. Biochem. Zool.*
378 **77**, 865-868 (2004).

379 56 Butler, P. J., Green, J. A., Boyd, I. L. & Speakman, J. R. Measuring metabolic rate in the
380 field: the pros and cons of the doubly labelled water and heart rate methods. *Funct.*
381 *Ecol.* **18**, 168-183 (2004).

382 57 Dlugosz, E. M. *et al.* Phylogenetic analysis of mammalian maximal oxygen consumption
383 during exercise. *J. Exp. Biol.* **216**, 4712-4721 (2013).

384 58 Norin, T. & Clark, T. D. Measurement and relevance of maximum metabolic rate in
385 fishes. *J. Fish Biol.* **88**, 122-151, doi:10.1111/jfb.12796 (2016).

386 59 Lynch, M. Methods for the analysis of comparative data in evolutionary biology.
387 *Evolution* **45**, 1065-1080, doi:10.2307/2409716 (1991).

388 60 Housworth, E. A., Martins, E. P. & Lynch, M. The phylogenetic mixed model. *Am. Nat.*
389 **163**, 84-96, doi:10.1086/380570 (2004).

390 61 Hadfield, J. D. & Nakagawa, S. General quantitative genetic methods for comparative
391 biology: phylogenies, taxonomies and multi-trait models for continuous and
392 categorical characters. *J. Evol. Biol.* **23**, 494-508 (2010).

393 62 Hinchliff, C. E. *et al.* Synthesis of phylogeny and taxonomy into a comprehensive tree of
394 life. *Proceedings of the National Academy of Sciences* **112**, 12764-12769,
395 doi:10.1073/pnas.1423041112 (2015).

396 63 Hadfield, J. D. MCMC methods for multi-response generalized linear models: the
397 MCMCglmm R Package. *Journal of Statistical Software* **33** (2010).

398 64 Schluter, D. Adaptive radiation along genetic lines of least resistance. *Evolution* **50**,
399 1766-1774 (1996).

400

401 **Fig. 1. Phylogenetic distribution of the genetic correlation (r_G) between metabolic rate**
402 **and body mass.** Species are (from top to bottom): African stonechat *Saxicola torquata*³³
403 (estimate for *Saxicola torquata axillaris* plotted above that for *Saxicola torquata rubicola*),
404 blue tit *Cyanistes caeruleus*³⁴, zebra finch *Taeniopygia guttata*³⁵, deer mouse *Peromyscus*
405 *maniculatus*³⁶, *Drosophila melanogaster*, *Drosophila serrata*, Cockroach *Nauphoeta cinerea*
406 (the estimate for females is plotted above that for males). Dotted lines correspond with values
407 of r_G of -1 and +1; the dashed line corresponds with $r_G = 0$. Data are shown \pm SE, the tree was
408 dated using www.timetree.org, endothermic species are coloured red, ectothermic species are
409 coloured blue.

410

411 **Fig. 2. Relationship between metabolic rate and body mass predicted by random**
412 **evolution.** Results are for 4000 tips evolving on a random tree, with a genetic correlation
413 between metabolic rate and body mass ($r_G = 0.78$, Fig. 1), a variance of 0.025 for log-
414 transformed body mass and a variance of 0.0183 for log-transformed metabolic rate,
415 calculated from the mean ratio of σ_{MR}^2 to σ_M^2 ; 0.73, see text for details). Orange lines are
416 density contours corresponding to (from inner to outer contour) the 50th, 80th, 90th, and 95th
417 percentiles. Dashed lines represent (from top to bottom) scaling exponents of 1, 0.75, and 0.5.

418

419 **Fig. 3. Empirical and simulated distributions of metabolic scaling exponents and mass-**
420 **independent variation in metabolic rate.** (a) Empirical scaling exponent of metabolic rate
421 for a range of species measured at rest (circles), while free living (squares), or during intense
422 activity (diamonds) shown \pm 95% CI. Groups that are predominantly endothermic are
423 coloured red, groups that are predominantly ectothermic are coloured blue. (b) Grey bars
424 depict the distribution of simulated scaling exponents under a model of random evolution
425 with a genetic correlation. The vertical dashed line represents the scaling exponent of $\frac{3}{4}$
426 predicted by several metabolic theories^{4,5,45,46}. (c) Standard deviation of the variation in
427 metabolic rate that is not explained by variation in body mass or temperature (residual
428 variation) for the relationships in (a). (d) Standard deviation of the variation in metabolic rate
429 that is not explained by variation in body mass for the relationships in (b).

430

431 **Fig. 4. Metabolic scaling relationships are not consistent with random evolution under**
432 **a genetic constraint alone.** In the upper panel, the black dots depict the combinations of
433 scaling exponents and residual standard deviation that are produced by 100,000 simulations
434 of the evolution of metabolic rate and body mass by random evolution under a genetic
435 constraint with genetic correlations modelled based on their empirical distribution (see text
436 for details). Orange lines are (inner to outer) 50th, 70th, 90th and 95th percentile density
437 contours of the 100,000 simulated exponents. Red and blue symbols represent empirical
438 metabolic scaling exponents for endotherms and ectotherms, respectively, for animals
439 measured at rest (circles), while free living (squares), or during intense activity (diamonds)
440 shown \pm 95% CI. The area enclosed by the dashed box in the upper panel is reproduced in the
441 lower panel for clarity.

442

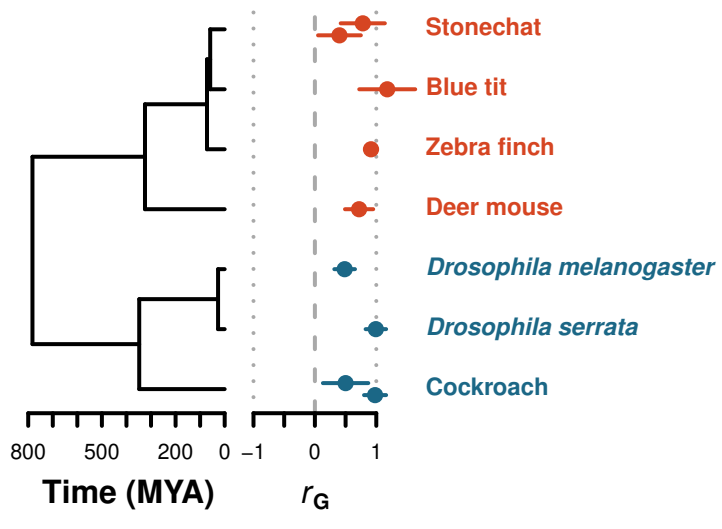
443 **Fig. 5. The phylogenetic diversity of metabolic rate and body mass.** (A) Ellipse outlining
444 the additive genetic ("breeding") values of individuals within a population. The shading in
445 panel a) depicts the fitness surface (darker shading corresponds with higher fitness)
446 describing the pattern of correlational selection on metabolic rate and body mass
447 hypothesized to generate the additive genetic correlation between metabolic rate and mass,
448 and to constrain the evolution of mass-independent metabolic rate. The long axis of the ellipse
449 is the direction of greatest genetic variance, \mathbf{g}_{\max} , which represents the genetic line of least
450 resistance⁶⁴ depicted by the dashed line. If the additive genetic variance-covariance matrix is
451 stable through time, evolution should proceed along the direction of \mathbf{g}_{\max} in the absence of
452 selection, yielding strongly correlated phenotypic values of metabolic rate and body mass, as
453 is observed for extant species (the lengths of the light grey bars in panel b are proportional to
454 \log_{10} -transformed body mass; dark grey bars are proportional in length to \log_{10} -transformed
455 resting metabolic rate). The observed additive genetic correlation between metabolic rate and
456 body mass for a range of animals (Fig. 1) predicts the among-species relationship between
457 metabolic rate and body mass (the slopes of the solid lines for the scaling of resting metabolic
458 rates in panels c-h) are the median simulated values for endotherms and ectotherms from Fig.
459 3b; colours correspond with clades in panel b).

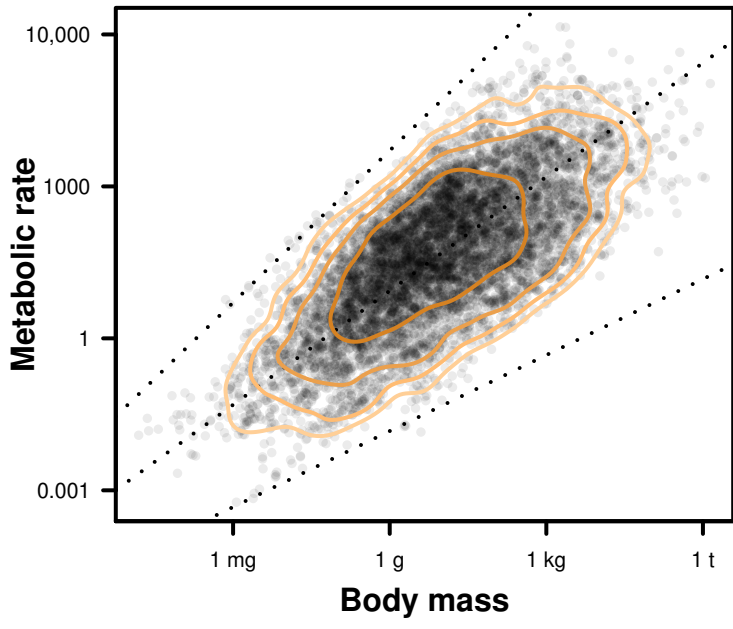
460

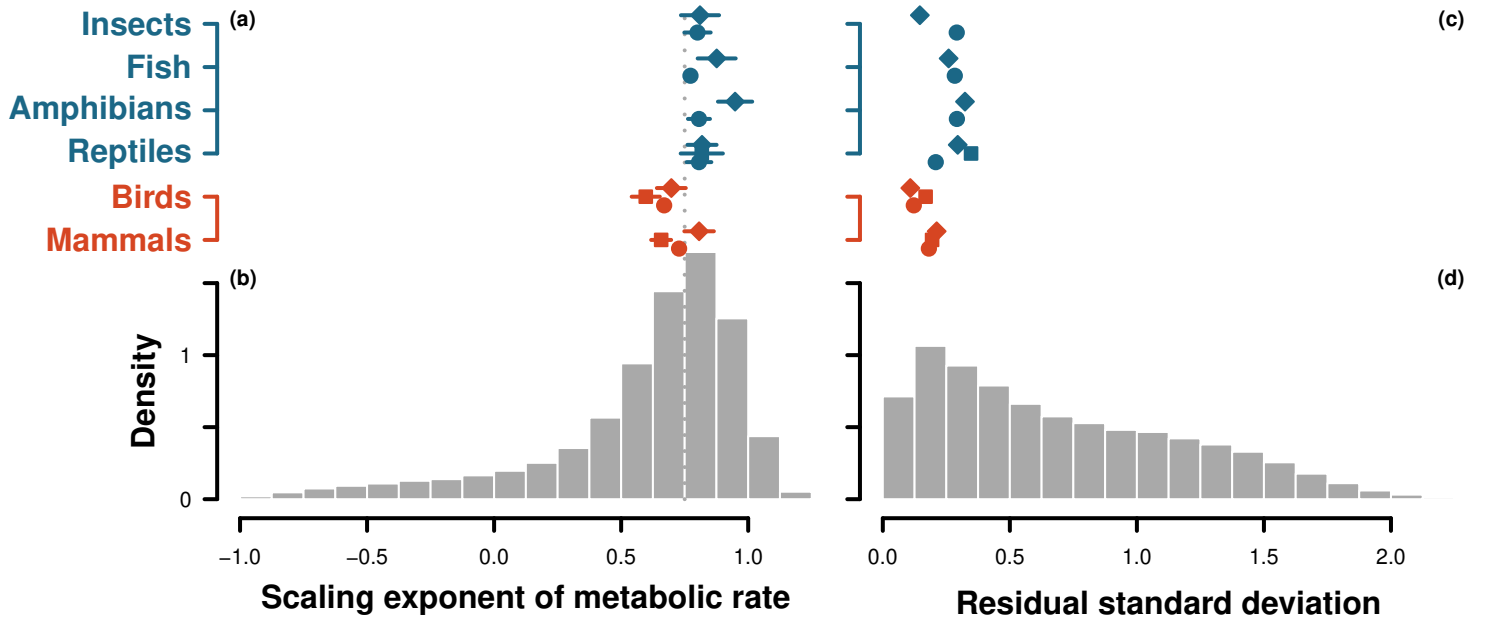
461

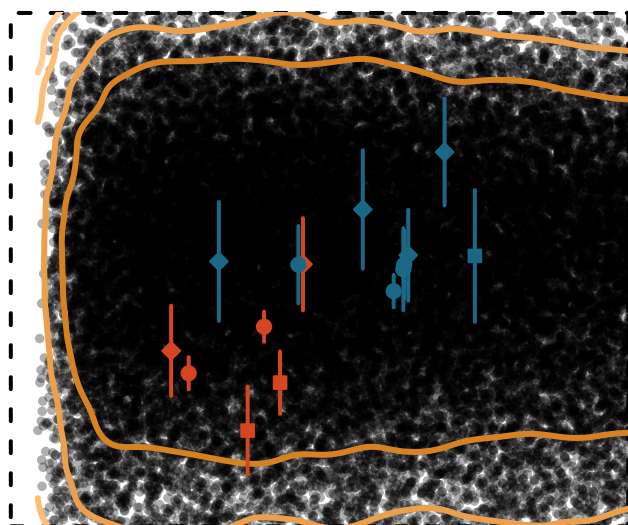
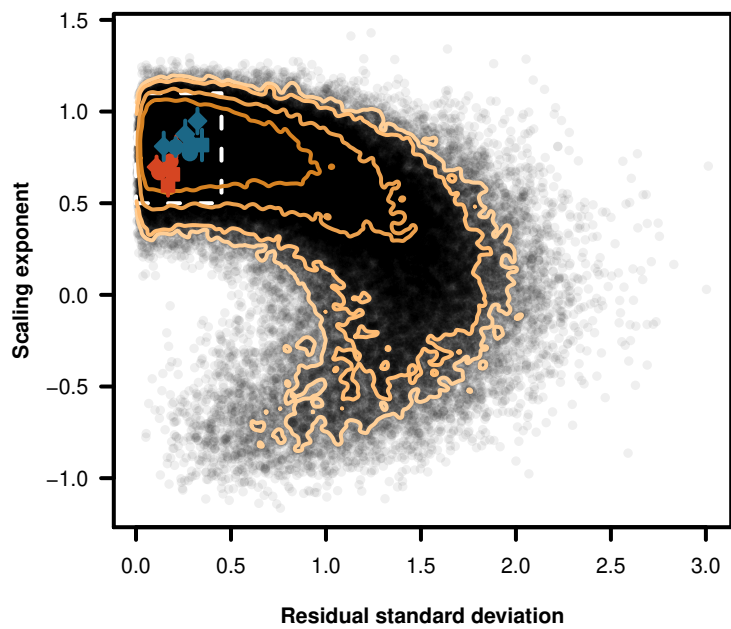
462

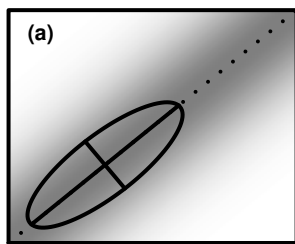
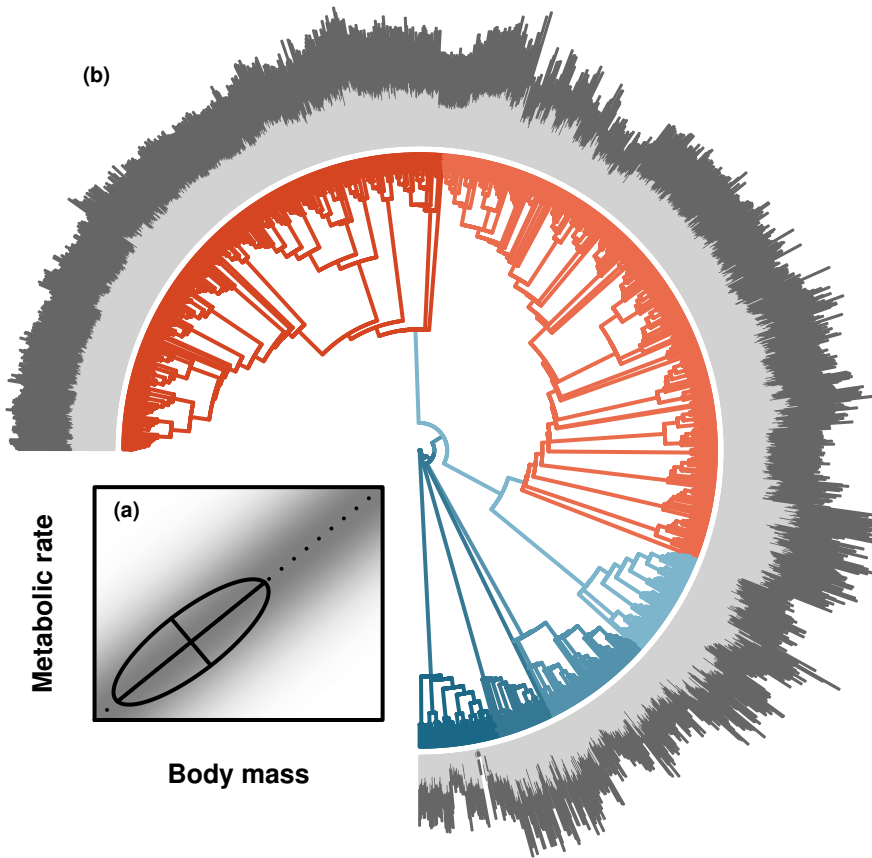
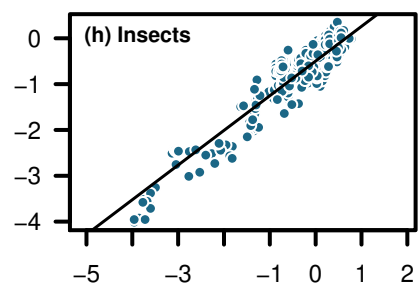
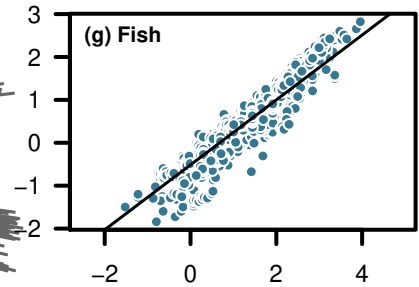
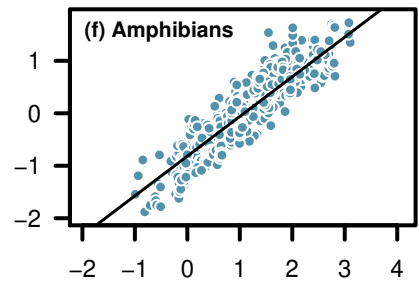
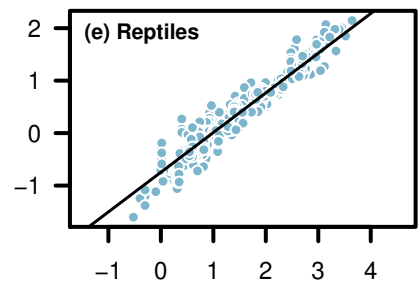
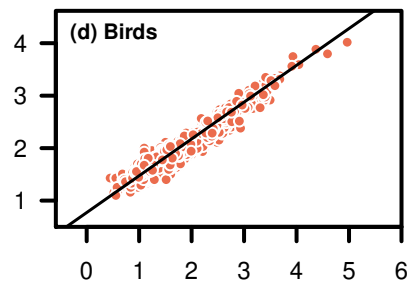
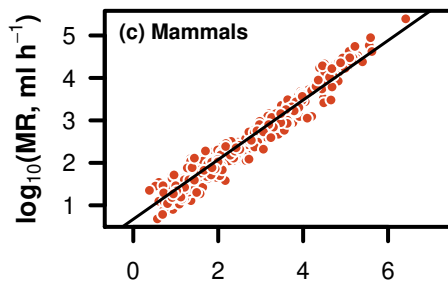
463











Body mass

$\log_{10}(\text{Mass, g})$